

9

Flexible Microfluidics for Wearable Electronics

Dachao Li¹, Haixia Yu², Zhihua Pu¹, Xiaochen Lai¹, Chengtao Sun¹, Hao Wu¹,
and Xingguo Zhang¹

¹Tianjin University, School of Precision Instruments and Optoelectronics Engineering, Department of Precision Instrument Engineering, State Key Laboratory of Precision Measuring Technology and Instruments, No. 92 Weijin Road, Tianjin 300072, China

²Tianjin University, School of Precision Instruments and Optoelectronics Engineering, Department of Biomedical Engineering, Tianjin Key Laboratory of Biomedical Detecting Techniques and Instruments, 92 Weijin Road, Tianjin 300072, China

9.1 Introduction

With the development of micro-electro-mechanical-systems (MEMS) technology, microfluidics is developed and widely used in various fields such as environment detection, cell biology, protein analysis, and gene engineering. Conventional microfluidic systems are generally fabricated using rigid materials such as silicon and glass. Rigid microfluidics requires complicated manufacturing procedures and expensive processing equipment; unfortunately, high integration is still very difficult. In recent years, flexible microfluidics is developed rapidly based on the fast development of materials and fabrication technologies. Flexible materials such as polymer, silicone elastomer, and fabric are used to fabricate the microfluidic system instead of conventional rigid materials. New fabrication technologies such as layer transfer and lamination, soft lithography, inkjet printing, and 3D printing are developed for flexible microfluidics. These flexible materials and fabrication technologies simplify the manufacturing procedures, cut the cost, and make flexible microfluidics multifunctional and highly integrated. In addition to flexibility, flexible microfluidics has the advantages of lightweight, conformability, portability, low cost, disposability, and easy integration. Therefore, flexible microfluidics is widely used, especially in wearable applications, including biosensing and motion sensing. In the next sections, more information about flexible materials (Section 9.2), fabrication technologies (Section 9.3), and applications of flexible microfluidics (Section 9.4) will be discussed, respectively.

9.2 Materials

Many materials have already been developed and used in flexible microfluidics. These materials can be divided into three classes: polymer, silicone elastomer,

and fabric. Each of these materials possesses inherent qualities compatible for different applications. For example, polymeric substrates are flexible, robust, and generally possess strong resistance to chemicals. Silicone elastomers are stretchable and conformable. The fabric is soft, absorbent, and breathable [1].

As the most popular polymer in microfluidics, polydimethylsiloxane (PDMS) has been widely used in flexible microfluidics due to its special characters, such as elasticity, transparency, biocompatibility, gas permeability, and ability to form conformal contact with surfaces. The Young's modulus of PDMS is approximately 2 MPa, although it can be modified by altering the ratio of PDMS base and curing agent or by changing the curing temperature. Consequently, a thin layer of PDMS can be soft, flexible, and deformable, similar to that of the skin. Furthermore, the structures fabricated with PDMS are hydrophobic, which could be altered by surface modifications. As such, PDMS substrates can be bonded easily and quickly to different kinds of materials without the need for adhesives.

Another thermoset polymer, which is usually used as the substrate of a flexible microfluidic chip, is polyimide (PI)[2]. Thermosetting PI is known for its thermal stability, good chemical resistance, excellent mechanical properties, and characteristic orange/yellow color. Polyimides compounded with graphite or glass fiber reinforcements have flexural strengths of up to 50 000 psi (340 MPa) and flexural moduli of 3 000 000 psi (21 000 MPa). Thermoset polymer matrix polyimides exhibit very low creep and high tensile strength. These properties are maintained during continuous use to temperatures of up to 232 °C (450 °F) and for short excursions, as high as 400 °C (752 °F) [3].

Other polymeric substrates include polyethylene terephthalate (PET), polyethylene (PE), polystyrene (PS), polyurethane (PU), polypropylene (PP), polycarbonate (PC), and cyclic olefin (co)polymers (COC/COP). These materials are thermoplastics, and they have been widely used in flexible printed electronics [4]. With fabrication techniques to achieve metallization of these polymeric substrates, these structures can serve as soft wires or even serve as sensors in various microfluidic chips. Another special kind of polymers is photosensitive resin, which can be cured under UV light. These photosensitive polymers are the fundamental materials of 3D printing, which is suitable for the fabrication of complex structures and multilayers or compound foils with more functionality.

Silicone rubber represents another class of materials for flexible microfluidics. It has already been well utilized in wearable devices due to its durability and excellent chemical resistance. Furthermore, its viscoelasticity matches that of the skin and can get the perfect fit with people's skin. For example, Ecoflex silicone rubber possesses an elastic modulus of approximately 125 kPa, which is similar to that of the skin. It can be stretched over 100% without plastic or permanent deformation. Similarly, the soft lithography technique can be used for silicone rubber substrates. To ensure mold release, precast silicone rubber should be peeled off the mask before it is fully cured. Electrical components can also be embedded in the silicone substrate.

Also, paper-based microfluidic devices fall within our definition of flexible microfluidics. In fact, not only is paper a potential candidate for flexible microfluidic chips but also it has already been successfully used as a substrate material for lateral flow assays, which are sold in billions of units in point-of-care

diagnostics [5]. Patterned paper can be used to manipulate micro-flow using capillary forces [6]. Paper is used when mainly capillary matrices are required. Suitable grades are often made of nitrocellulose such as chromatographic paper.

As an emerging extension, the fabric or textile-based microfluidics utilizes a wicking force similar to that in the paper that is produced by hydrophilic yarns (e.g. cotton yarns) to direct biological reagents along with the fibrous structure. This structure affords the aforementioned operational capacities of interfacial microfluidics while providing a low-cost and scalable solution based on well-established traditional textile manufacturing techniques such as automatic weaving, knotting, and stitching. In addition, textile-based microfluidics is inherently more durable and could be easily woven onto clothes and accessories. However, in order to control bio-fluidic transport, specialized channels have to be fabricated. Chemical treatment and photolithographic means are usually used for surface modification to alter textile hydrophobicity. Taking advantage of the difference in wetting properties, liquid droplets can be self-propelled in an open-channel configuration under Laplace pressure gradients. Other than fluidic transport, electrical coating of textile or e-textile is necessary for providing electrochemical reactions and data transmission. Here, secondary processes such as dip coating and stencil printing have been employed to achieve electrically conductive fabric.

9.3 Fabrication Technologies

The fabrication technologies used for microfluidic systems have evolved to improve functionality. Early microfluidic systems were manufactured from glass and silicon. However, glass/silicon fabrication requires complex etching processes and is fundamentally limited to very planar, passive devices. To form an integrated microfluidic system, a micro/nanostructured layer is bonded to a microchannel layer. Various micro/nanofabrication techniques can be used for manufacturing integrated microfluidic systems on flexible substrates, such as a polymer, silicone elastomer, and fabric. In the first part of this section, fabrication methods of traditional microfluidic devices made by polymer and silicone elastomer are introduced, including layer transfer and lamination, soft lithography, inkjet printing, and 3D printing; in the second part, the processing methods of open-surface microfluidics made by fabric are introduced.

9.3.1 Layer Transfer and Lamination

The layer transfer and lamination technique can be used to fabricate flexible microfluidic channels in various shapes and with a wide range of dimensions. High bond strengths can be achieved by cure cycle adaptation, and the microchannels can be combined with metallization layers to fabricate electrodes inside and outside the channels.

Metz et al. present a method to fabricate flexible microfluidic devices using layer transfer and lamination technique [2]. The device is micromachined on

a carrier substrate. The resulting structures can be removed from the carrier substrate by using a release technique based on the anodic metal dissolution of aluminum. On the aluminum surface, a 5–20 μm thick layer of photosensitive polyimide is applied, photostructured and cured (Figure 9.1a). Subsequently, a layer of titanium-platinum is sputtered on the substrate and structured by dry etching using a positive photoresist as etch mask (Figure 9.1b). The second layer of photosensitive polyimide is spin-coated to define the channel walls and insulate the metallization layer where embedded metallic conductors are desired (Figure 9.1c). On the surface of Mylar™ foil on the second substrate, a 5–20 μm thick layer of photosensitive polyimide is spin-coated (Figure 9.1d). Following a soft bake step on a hotplate, the second substrate is flipped over and bonded to the open channel structures on the first wafer by lamination (Figure 9.1e). After peeling off the Mylar™ foil (Figure 9.1f), the top layer of polyimide is photostructured and the devices are again cured under nitrogen at 350 °C for one hour (Figure 9.1g). During the anodic metal dissolution process of aluminum, the gold remains on the substrate due to the difference in the electrochemical potential compared with aluminum and ensures electrical contact until the structures are released (Figure 9.1h). The fabricated device

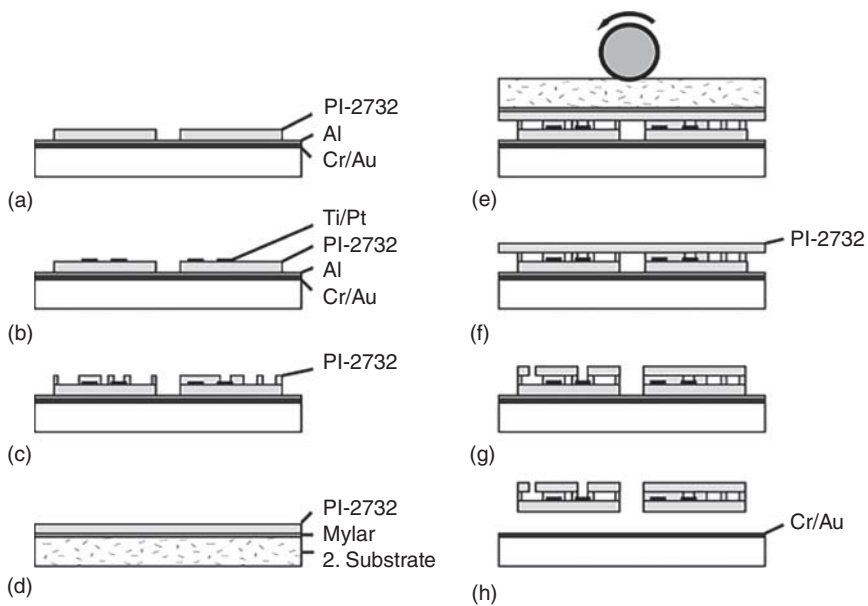


Figure 9.1 Fabrication steps for polyimide-based microfluidic devices. (a) Photolithography. (b) Sputtering and dry etch. (c) Photolithography. (d) Cover layer preparation. (e) Cover layer bonding. (f) Substrate and Mylar removal. (g) Photolithography and Cure. (h) Final release. Source: (a–h) Metz et al. 2001 [2]. Copyright 2001, Reproduced with permission of Wiley-VCH Verlag GmbH & Co. KGaA; Liaw et al. 2012 [3]. Copyright 2012, Reproduced with permission of Wiley-VCH Verlag GmbH & Co. KGaA; Wang et al. 2016 [4]. Copyright 2016, Reproduced with permission of Wiley-VCH Verlag GmbH & Co. KGaA; Schubert-Ullrich et al. 2009 [5]. Copyright 2009, Reproduced with permission of Wiley-VCH Verlag GmbH & Co. KGaA; Martinez et al. 2007 [6]. Copyright 2007, Reproduced with permission of Wiley-VCH Verlag GmbH & Co. KGaA.

can be used for flexible fluidic and electrical connectors, and for many other applications in medical, chemical, and biological research.

9.3.2 Soft Lithography

Soft lithography is a popular method for rapid prototyping of microfluidic devices. The majority of reported laboratory-scale prototypes were fabricated with this method. Soft lithography has provided a low-expertise route toward micro/nanofabrication and plays an important role in microfluidics, ranging from simple channel fabrication to the creation of micropatterns onto a surface or within a microfluidic channel. A low-cost and simple method is to fabricate a solid matrix by using lithography to construct the SU-8 layer, as shown in Figure 9.2a. Using the SU-8 master mold, a PDMS microfluidic device could be fabricated following the procedures in Figure 9.2b. The PDMS mixture is poured into the master batch and then solidified for several hours at relatively low temperatures (60–80 °C). After stripping and surface treatment with oxygen plasma, the structured PDMS film is contacted with clean glass, silica, or another surface activated PDMS [7]. Instead of drilling the reservoirs and entry holes in the PDMS layer, glass posts could be placed on the SU-8 mainframe to determine the access to the holes and reservoirs.

Soft lithography is also a direct pattern transfer technique. The term “soft” refers to an elastomeric stamp with patterned relief structures on its surface. PDMS has been used successfully as the elastomeric material. Two soft lithographic methods are introduced to fabricate micro/nanopatterns onto a surface

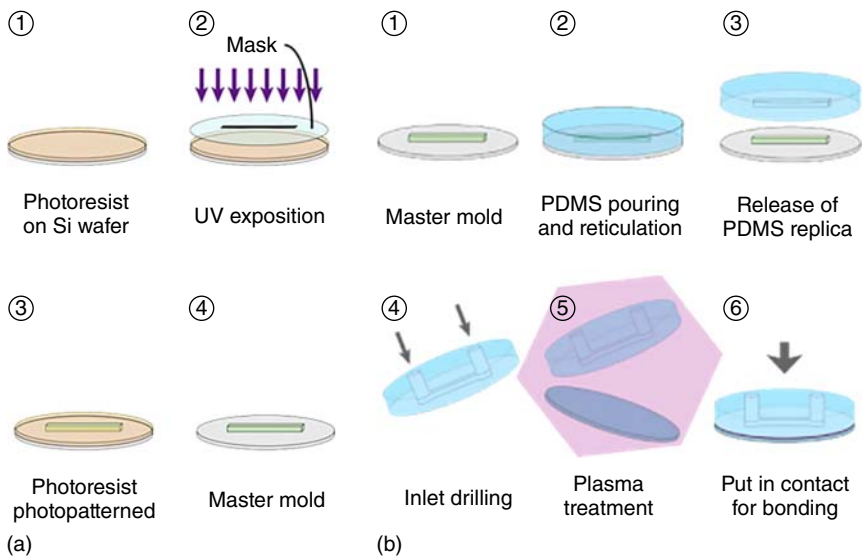
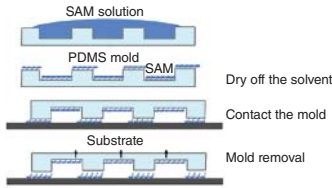
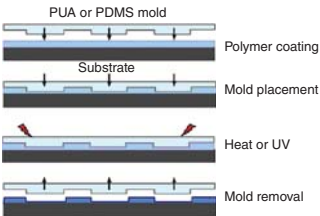


Figure 9.2 Fabrication method of the microfluidic device by soft lithography. (a) The fabrication process of the master mold and the (b) fabrication process of the microfluidic device using the master mold. Source: (a, b) Nguyen 2008 [7]. Copyright 2008, Reproduced with permission of Elsevier.

Table 9.1 Soft lithographic methods for the fabrication of micro/nanopatterns.

| | Contact printing | Capillary molding |
|-------------|---|---|
| Mold | Soft mold PDMS Hard PDMS(h-PDMS) | PDMS PUA |
| Resolution | ~500 nm ~50 nm with h-PDMS | ~50 nm with PUA mold |
| Application | 1. Channel fabrication 2. Direct printing of biological molecules | 1. Channel fabrication 2. Fabrication of micro/nanostructures |
| Process |  <p>1. SAM solution 2. PDMS mold 3. Dry off the solvent 4. Contact the mold 5. Substrate 6. Mold removal</p> |  <p>1. PUA or PDMS mold 2. Polymer coating 3. Substrate 4. Mold placement 5. Heat or UV 6. Mold removal</p> |

Source: Kim et al. 2008 [8]. Copyright 2008, Reproduced with permission of WILEY-VCH Verlag GmbH & Co. KGaA.

or within a microfluidic channel: contact printing and capillary molding. Contact printing generates a nonstructured, chemically modified surface, while capillary molding fabricates a topographically modified physical micro/nanostructure [8] (Table 9.1).

9.3.3 Inkjet Printing

Photolithography relies on photomasks and photosensitive materials, which limits the flexibility of lithography. Printing technology, as a kind of high-efficiency technology, has shown tremendous application prospects in pattern-based fabrication and functional materials fabrication of electronic devices, plate making, and microchannels.

A simple method for fabricating microchannels is presented based on inkjet printing liquid templates [9]. By using a temperature-sensitive ink, the shape of the liquid template can be well controlled. Figure 9.3 shows the fabrication process of a typical microfluidic reactor by inkjet printing. The first step is to pour the prepolymer mixture into the container. The Y pattern, which acts as a template, is printed onto the surface of the prepolymer mixture and spontaneously wrapped in the prepolymer mixture. The prepolymer mixture is then thermally cured. At the same time, the liquid template evaporates, leaving the Y microchannel in the matrix. A typical microfluidic reactor is obtained by stripping the matrix from the container.

9.3.4 3D Printing

The advent of soft lithography allowed for an unprecedented expansion in the field of microfluidics. However, the vast majority of microfluidic devices are still

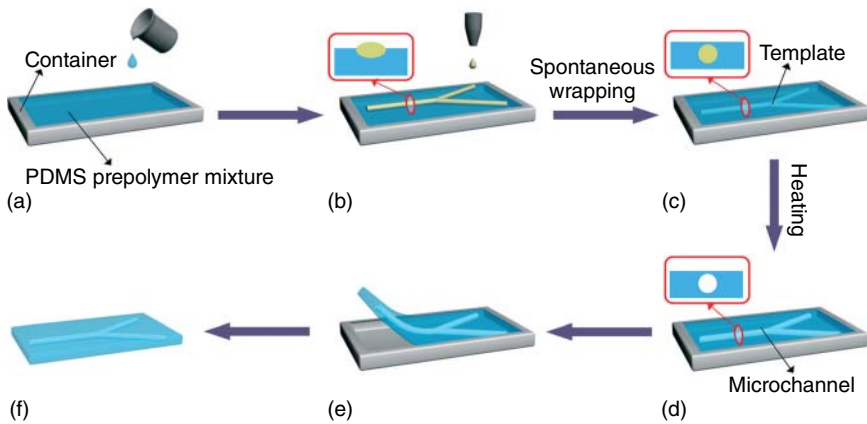


Figure 9.3 Fabrication process of a typical microfluidic reactor by inkjet printing. (a) Pouring the PDMS prepolymer mixture into a Container. (b) Printing a Y-shape pattern on the surface of the prepolymer mixture. Inset: relative position sketch of the pattern and prepolymer mixture surface. (c) Standing for a few seconds to allow the pattern to be wrapped spontaneously. Inset: relative position sketch of the pattern and prepolymer mixture surface. (d) After heating the prepolymer mixture with the liquid template, the prepolymer mixture thermally cures and the liquid template evaporates, leaving the microchannel in the PDMS matrix. Inset: section sketch of the microchannel in the matrix. (e) Peeling off the fabricated PDMS matrix with microchannel. (f) The typical microfluidic reactor in the PDMS matrix. Source: Guo et al. 2015 [9]. Copyright 2015, Reproduced with permission Royal Society of Chemistry.

made with extensive manual labor, are tethered to bulky control systems, and have cumbersome user interfaces, which all render commercialization difficult. On the other hand, 3D printing has begun to embrace the range of sizes and materials that appeal to the developers of microfluidic devices. For 3D printing, prior to fabrication, a design is digitally built as a detailed 3D computer-aided design (CAD) file. The design can be assembled in modules by remotely collaborating teams, and its mechanical and fluidic behavior can be simulated using finite-element modeling. As structures are created by adding materials without the need for etching or dissolution, the processing is environmentally friendly and economically efficient.

9.3.4.1 3D Printing Sacrificial Structures

3D printing technology is suitable for many kinds of materials. For example, soluble materials could be printed and act as the sacrificial template for microfluidic device fabrication. Here, an easy two-step acrylonitrile butadiene styrene (ABS) scaffold-removal method is presented for achieving 3D, multilayer, intricate, micrometric channels in a single block of PDMS. Using the scaffold-removal fabrication method, external components, such as heating elements, electronics, or radio frequency (RF) circuitry, can be embedded directly in microfluidic devices.

Figure 9.4 shows the schematic representation of the ABS scaffold-removal fabrication method for manufacturing microfluidic devices. An ABS plastic scaffold is modeled or 3D printed in the desired shape. Consecutively, it is suspended in PDMS with or without the addition of external components and then the polymer is cured. Finally, the scaffold is removed by immersion in acetone, creating the microfluidic channels [10].

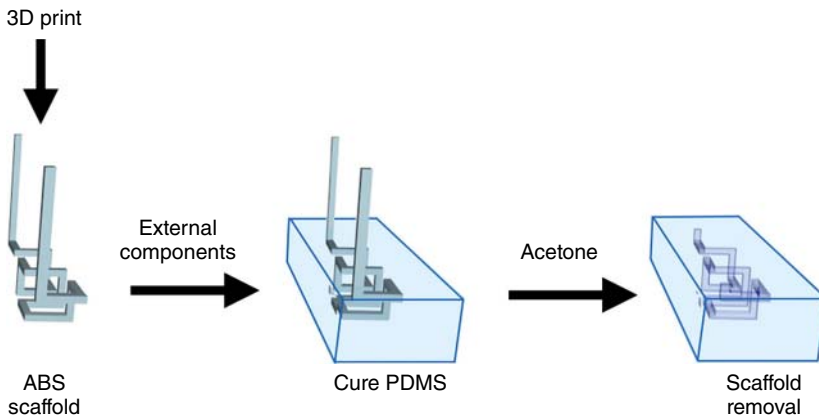


Figure 9.4 Schematic representation of the ABS scaffold-removal fabrication method for microfluidic devices. Source: Saggiomo and Velders 2015 [10]. Copyright 2015, Reproduced with permission John Wiley & Sons.

9.3.4.2 3D Printing Templates

Direct printing of flexible microfluidic device, implemented by micro-stereolithography, has traditionally required expensive infrastructure, whereas the emergence of affordable 3D printers has the potential to grant broader access to custom-made microstructures, by minimizing resources and fabrication skills.

As shown in Figure 9.5, Comina et al. present a fabrication method of conventional lab-on-a-chip devices made by 3D printer [11]. The template is designed by CAD and printed with a commercial micro-stereolithography 3D printer. The printed templates replace clean room and photolithographic fabrication resources and deliver resolutions of 50 μm . Whereas the templates are smooth enough, it can direct transfer and proper sealing to substrates. After protecting the surface of templates, the polymer is directly cast on the 3D printed templates with no additional processing cost or effort. This simplified method promotes access to build flexible device configurations with minimal fabrication requirements and provides a versatile flexible device development platform with a 3D printer.

9.3.5 Fabrication of Open-Surface Microfluidics

Open-surface and interfacial microfluidics, where one or more gas/liquid interfaces exist as boundary conditions, is the emerging trend in microfluidics from which several new and flexible operations have been established, including self-propelled motion, three-dimensional connectivity, open sample accessibility, direct reactivity, and readability, in addition to conventional microflow manipulations.

9.3.5.1 Fabrication of Paper-Based Microfluidic Device

The paper-based microfluidics diagnostic device is inexpensive, robust, lightweight, and independent of supporting infrastructure. Martinez et al.

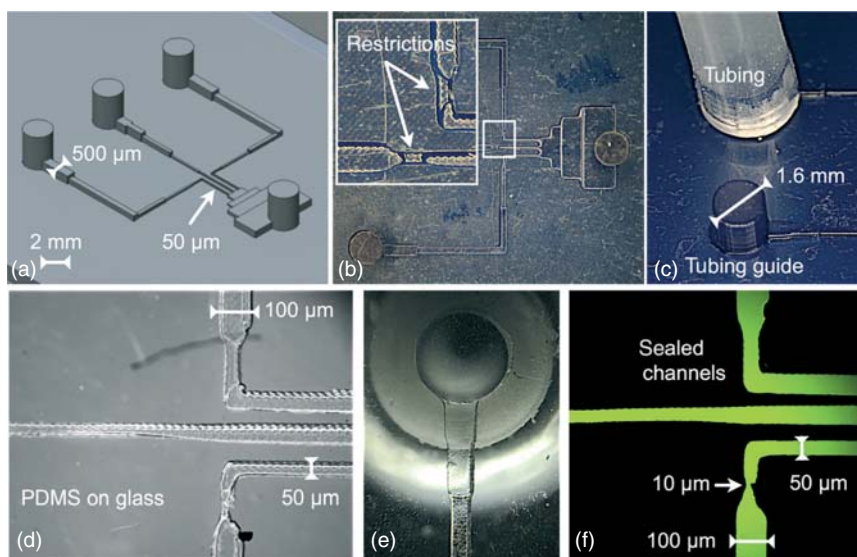


Figure 9.5 Lab-on-a-chip device fabricated using templates printed with 3D printer. (a) CAD with 50 μm and 2 mm features combined in the same design. (b) 3D printout of the structure in (a). The inset highlights hindrances developed at the 50–100 μm channel step. (c) Image of the printed pillar guides used to integrate silicone tubing in the PDMS structure. (d) PDMS device assembled on a glass substrate showing no texture at the PDMS–glass interface. (e) Microscopic image of tubing connected to a 500 μm channel. (f) Epi-fluorescence microscopic image of PDMS structure filled with fluorescein solution. Source: (a–f) Comina et al. 2014 [11]. Copyright 2014, Reproduced with permission of Royal Society of Chemistry.

described a new type of paper-based device, which makes the paper layer into the hydrophilic channel, hydrophobic wall, and ribbon structure, and connects the channels on different paper layers with tape patterned holes [12]. These devices extend the paper-based analysis from simple one-dimensional lateral flow systems to 3D devices with complex microfluidic paths, and significantly expand the capabilities of low-cost analysis systems.

As shown in Figure 9.6, the 3D paper-based flow system is produced by stacking alternating paper and waterproof double-sided adhesive tape. Patterned hydrophobic polymers on paper delineate channels for fluid transverse movement, impermeable double-sided tape layers separate channels in adjacent paper layers, and holes cut into the tape allow fluid to flow vertically. The paper is patterned with SU-8 photoresist by being impregnated with photoresist, dried, exposed to ultraviolet light through a transparent mask, and developed with acetone and isopropanol. The adhesive tape is patterned with a laser cutting machine, which can also be manually patterned with a puncher. Then the layers of paper and adhesive tape are stacked together. A layer of adhesive tape is attached to the patterned paper layer. The holes on the adhesive tape are filled with a paste made from cellulose powder and water. The protective film is removed from the adhesive tape and second layers of paper placed on the second surface. This stacking-paper-tape-paper-tape process is repeated as needed to complete the device, and a reproducible method for manufacturing the device is provided.

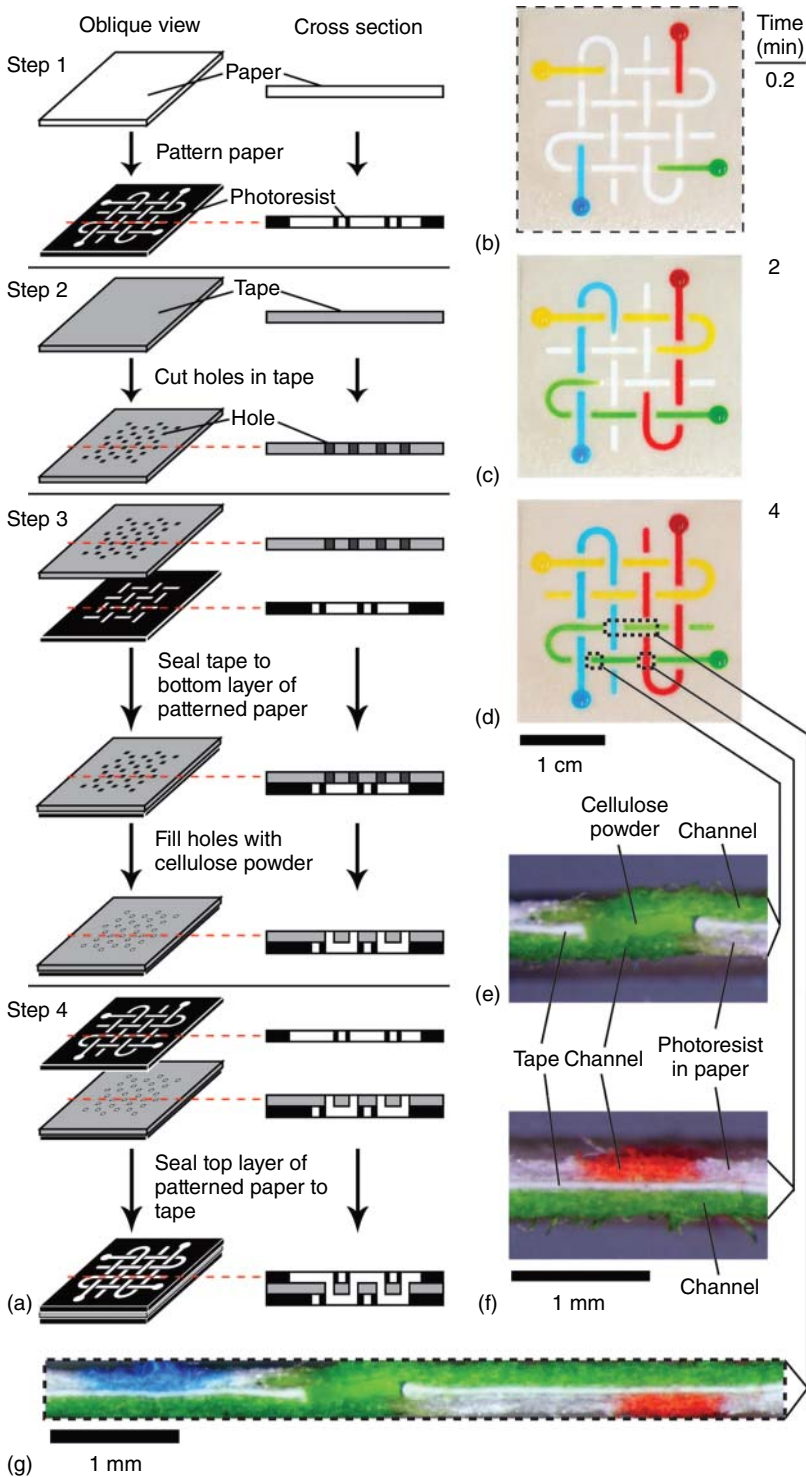


Figure 9.6 Three-dimensional microfluidic devices fabricated in layered paper and tape. Source: Martinez et al. 2008 [12]. Copyright 2008, Reproduced with permission of PNAS.

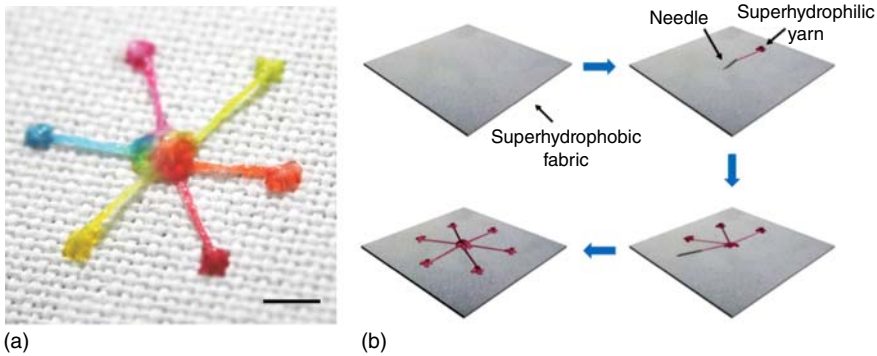


Figure 9.7 The fabrication process of MST with multi-inlet-single-outlet design. (a) A multi-inlet-single-outlet design on the MST platform using the autonomous interfacial transport concept. (b) The fabrication process of MST with multi-inlet-single-outlet design. Source: Xing et al. 2013 [13]. Copyright 2013, Reproduced with permission of Royal Society of Chemistry.

9.3.5.2 Fabrication of Textile-Based Microfluidic Device

The interfacial microfluidic concept has been extended to textile-based structures and surfaces. The textile-based microfluidics utilizes a similar wicking force to that in paper that is produced by hydrophilic yarns (e.g. cotton yarns) to direct biological reagents along the fibrous structure, which affords the aforementioned operational capacities of interfacial microfluidics while providing a low-cost and scalable solution based on well-established traditional textile manufacturing techniques such as automatic weaving, knotting, and stitching.

In a recent study, a novel interfacial microfluidic transport principle is used to drive 3D liquid flow on a micropatterned superhydrophobic textile (MST) platform in a more autonomous and controllable manner [13]. Specifically, the MST system utilizes the surface tension-induced Laplace pressure to facilitate liquid motion along the hydrophilic yarn, in addition to the capillarity present in the fibrous structure. The fabrication of MST is simply accomplished by stitching hydrophilic cotton yarn into a superhydrophobic fabric substrate, from which well-controlled wetting patterns are established for interfacial microfluidic operations. The geometric configurations of the stitched micropatterns, e.g. the lengths and diameters of the yarn and bundled arrangement, can all influence the transport process (Figure 9.7).

9.4 Applications

With the fast development of flexible materials and fabrication methods, the combination of fluid manipulation and flexible electronics promotes the application of functional microfluidics, e.g. wearable microfluidics for biosensing and health care. Typically, wearable microfluidics detects biofluids by the following procedures: (i) collect the biofluids, (ii) transfer biofluids to detection site, and (iii) perform detection. Blood, serum, sweat, interstitial fluid (ISF), saliva,

tears, mucus, semen, and stools are usually the source of the biofluids [14]. Especially, sweat is the analyte most commonly processed. In addition, wearable microfluidics could also be used for motion sensing of human bodies.

9.4.1 Wearable Microfluidics for Sweat-Based Biosensing

Sweat contains plenty of physiological information. Sweat sensors integrated into wearable microfluidics offer methods for gaining molecular-level insight into the dynamics of our bodies. Many wearable sweat sensors have been developed in recent years and combined with different form factors, substrates, and detection mechanisms.

Kim et al. used superabsorbent polymer (SAP) valves and colorimetric sensing reagents as the enabling components of soft, skin-mounted microfluidic devices designed to capture, store, and chemically analyze sweat released from eccrine glands [15]. The valving technology guided the flow of sweat from an inlet location into a collection of isolated reservoirs, in a well-defined sequence. Figure 9.8 shows the schematic illustration of the structure of the chrono-sampling epidermal microfluidic device for sweat chloride monitoring. The channel system was designed into a double layer geometry that separately supported the microfluidic channels and valves. A collection of active valves based on SAP materials and

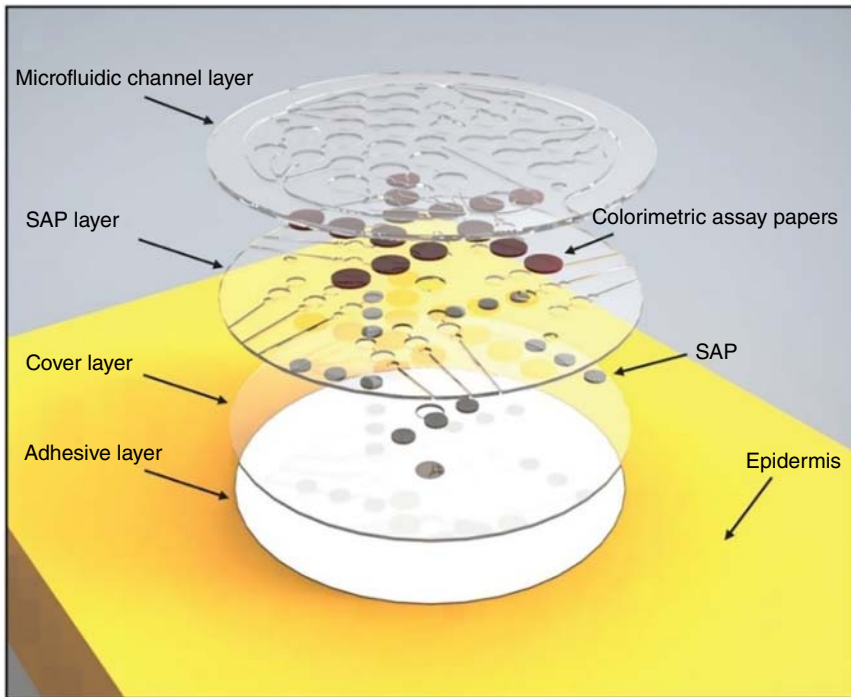


Figure 9.8 The schematic illustration of the structure of the chrono-sampling epidermal microfluidic device for sweat chloride monitoring. Source: Kim et al. 2018 [15]. Copyright 2018, Reproduced with permission of John Wiley & Sons.

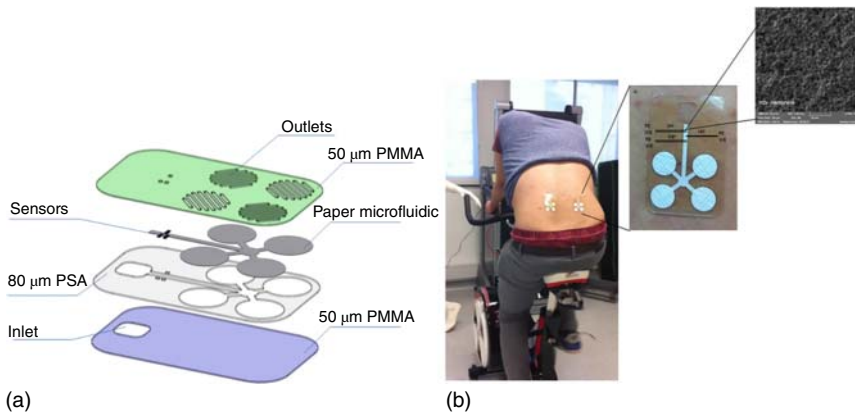


Figure 9.9 (a) Schematic representation of the fabrication steps of the microfluidic chip; (b) photograph of the chip attached to the body and scanning electron microscopic (SEM) image (magnification 2.00 k \times) photograph of IrOx pH sensor membrane on top of a 50 μ m Pt wire . Source: (a, b) Anastasova et al. 2017 [17]. Copyright 2017, Reproduced with permission of Elsevier.

passive valves exploited tailored hydrophobic and hydrophilic surface chemical functionalization on the surfaces of the channels. The active valves are used to close the inlets and outlets of each reservoir. The passive valves are used to guide the flow directionality.

Koh et al. presented a series of materials and device designs for soft, flexible, and stretchable microfluidic systems to establish sweat monitoring technologies [16]. The sweat can spontaneously get through a microfluidic network and a set of reservoirs by access points. Colorimetric fashions were used to analyze markers such as chloride and hydronium ions, glucose, and lactate. In addition, the wireless communication electronics integrated into the wearable microfluidic systems can intimately and robustly bond to the surface of the skin without chemical and mechanical irritation.

Anastasova et al. presented a fully integrated flexible microfluidic system for continuous, simultaneous, and selective measurement of sweat metabolites, electrolytes, and temperature [17]. The flexible microfluidic system can transmit information wirelessly for ease of collection and storage, with the potential for real-time data analytics. Figure 9.9 shows the schematic representation of the fabrication steps of the microfluidic chip and a photograph of the chip attached to the body.

Benito-Lopez et al. presented a wearable, robust, flexible, and disposable microfluidic chemical barcode platform [18]. The platform incorporated novel ionic liquid polymer gels (ionogels). The device can monitor the sweat pH in real time during an exercise period. The microfluidic structure makes the fresh sweat continuously pass through the sensing area and that ensures continuous real-time analysis and immediate feedback regarding sweat composition.

Yang et al. reported a wearable microfluidic platform to measure the flow rate on a patterned fabric surface referred to as digital droplet flowmetry (DDF). The platform was made by using conventional fabric materials and laser

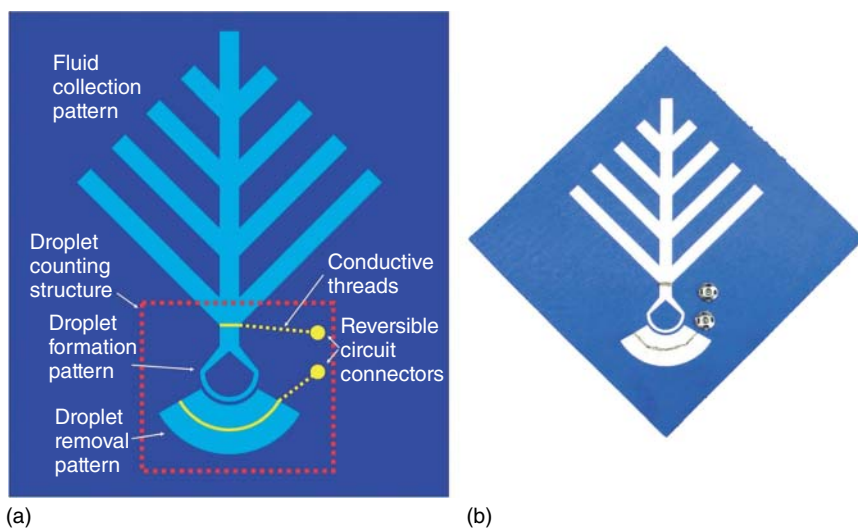


Figure 9.10 (a) Illustration and (b) a prototype of the wearable digital droplet flowmetry. Source: Yang et al. 2017 [19]. Copyright 2017, Reproduced with permission of Royal Society of Chemistry.

micromachining [19]. The proposed wearable DDF can collect and measure continuous perspiration with high precision (96% on average) in a real-time fashion. Moreover, the proposed DDF platform can be conveniently integrated with regular apparel or a wearable device and has potential to be applied to dynamic removal, collection, and monitoring of biofluids for various physiological and clinical processes. Figure 9.10 shows the illustration and prototype of wearable DDF.

9.4.2 Wearable Microfluidics for ISF-Based Biosensing

ISF is another source for molecular-level detection of physiological information of the human body. Li's group has done a great deal of work on transdermal extraction of ISF by flexible microfluidics providing a new way for continuous blood glucose monitoring [20–24]. Yu et al. fabricated a five layers PDMS microfluidic chip for ISF transdermal extraction, collection, and measurement toward the application of continuous and real-time glucose monitoring [20]. The photograph of the chip integrated a fiber-optic surface plasmon resonance (SPR) sensor for glucose concentration measurement is shown in Figure 9.11 [21]. Wu et al. proposed a new method of manufacturing stable microelectrodes on PDMS by inkjet printing and fabricated a three-electrode electrochemical sensor for glucose detection in a microfluidic system based on PDMS [22]. Figure 9.12 shows the optical image of the three-electrode electrochemical sensor fabricated on PDMS. In order to improve the performance of the electrochemical sensors, Pu et al. modified the working electrode of the sensor with graphene and gold nanoparticles by inkjet printing to form a composite nanostructure [23]. Pu et al. also reported an all-inkjet-printed flexible epidermal microfluidic system, which

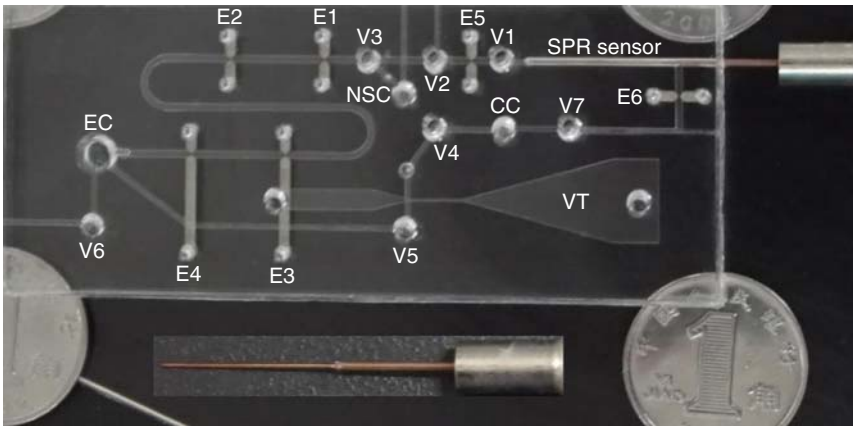


Figure 9.11 Optical image of the flexible microfluidic chip integrated with a fiber-optic SPR sensor for continuous ISF transdermal extraction and glucose concentration monitoring. Source: Li et al. 2016 [21]. Copyright 2016, Reproduced with permission of American Institute of Physics.

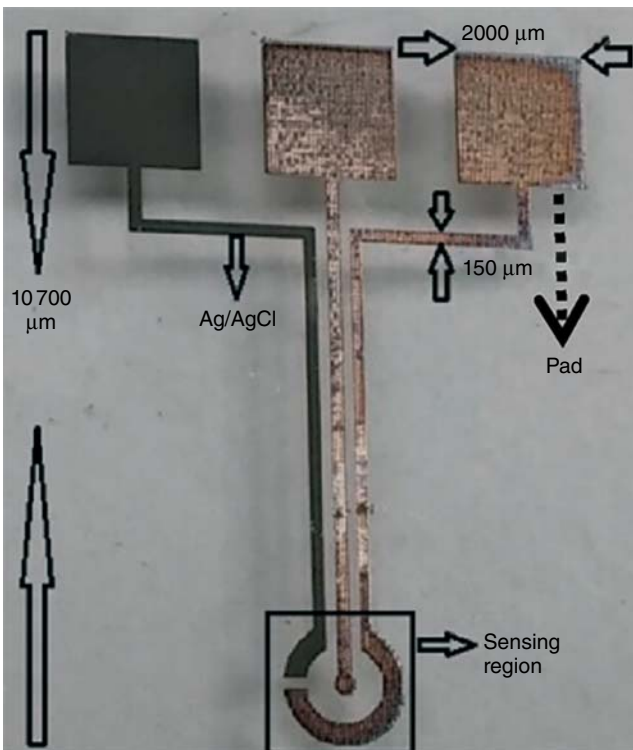


Figure 9.12 Optical image of a three-electrode electrochemical sensor on PDMS after silver chloride (black) formation. Source: Wu et al. 2015 [22]. Copyright 2015, Reproduced with permission of Royal Society of Chemistry.

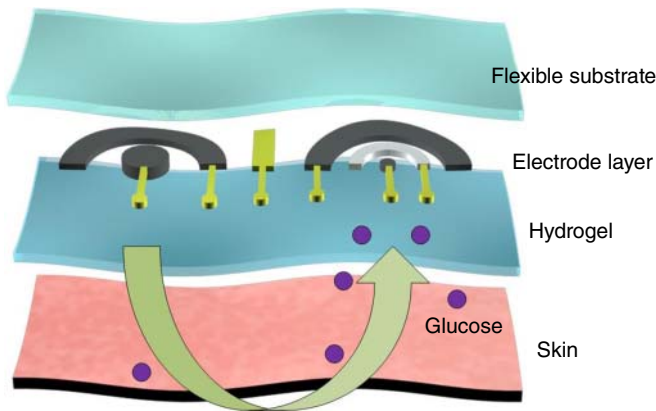


Figure 9.13 Photographs of the flexible epidermal microfluidic system attached to the skin [24].

consists of seven disposable four-electrode measuring array units [24]. Two of the electrodes are used to form epidermal microfluidic channels through the skin to transdermally extract ISF with glucose molecules by ions transportation. Figure 9.13 shows photographs of the flexible epidermal microfluidic system attached on the skin.

9.4.3 Wearable Microfluidics for Motion Sensing

Wearable microfluidics is also used for motion sensing of human bodies. Liquid metal in the microchannel is used as pressure sensor. Yeo et al. developed a liquid-based thin-film microfluidic tactile sensor, which has high flexibility, robustness, and sensitivity [25]. A highly conductive metallic liquid, eutectic gallium indium (eGaIn), functionalized the microfluidic sensor. The principle of the sensor is that the micro-deformation of the pressure sensor results in fluid displacement and that changes the electrical resistance. Figure 9.14 shows the photographs of the sensors. The sensors were multiplexed to detect forces at multiple regions of the hand.

Jiao et al. developed all-flexible strain sensors made of graphene, microfluidic liquid metal, and stretchable elastomer. Liquid metal was introduced into



Figure 9.14 Positions of the sensors: index finger, thumb, and palm region. Source: Yeo et al. 2016 [25]. Copyright 2016, Reproduced with permission of Royal Society of Chemistry.

microfluidic channels for wiring inside the devices [26]. Graphene was patterned inside of the liquid metal containing elastomer. The fluid eGaln made the microfluidic electrical wires to flow and reshape without cracks and fatigue in response to the sensor deformation during mechanical sensing. The graphene sensor was able to track the angular motion of a human wrist.

Chossat et al. designed and manufactured a kind of soft artificial skin with an array of embedded soft strain sensors. The sensor can detect various hand gestures by measuring joint motions of the five fingers [27]. Two different liquid conductors, an ionic liquid and a liquid metal, were filled into microchannels, which were made of a hyperelastic elastomer material.

9.4.4 Other Flexible Microfluidics

9.4.4.1 Soft Robotics

Apart from the abovementioned sensing applications, flexible microfluidics has been employed in soft actuating devices, namely the soft robotics. Pioneered by the Whitesides group, soft robotics has expanded to a wide range of use from giant robots for industrial applications to miniaturized robots for surgery and drug delivery. The soft robots have several advantages over rigid robots, such as the shock-free contact to objects, safe human–machine interaction, and simple gripping mechanism.

The dominant actuation strategy of soft robotics is pneumatic actuation. Figure 9.15 illustrates the operating mechanisms of soft robots that are pneumatically actuated by a fluid. Adding materials to introduce asymmetries enables the design of structures that deform into specific shapes [28].

The soft robotics has a large range of applications. For instance, soft robots could be used in the food industry for handling brittle objects. In clinical applications, soft robotic assistance is beneficial for delivering therapy and for restoring motor functionality [29]. In various works, the soft robots, integrated with sensing components, are used as rehabilitation assistance [30] and prostheses [31]. The combined abilities of sensing and actuating built on an entirely soft and flexible platform are advantageous for stroke and rehabilitation patients. Apart from macroscopic applications, soft robots are also reported to be capable of handling delicate tasks, such as soft robots for surgery [32].

9.4.4.2 Drug Delivery

Drug delivery is another fascinating application of flexible microfluidics. Although drug patches have been successfully developed previously, the efficacy of drug release over time remains a challenge due to its concentration effect. Microfluidics-enabled drug patch may overcome this problem by ensuring consistent drug dispensing over prolonged periods. Furthermore, the possibility of fabricating microneedles allows painless drug administration and ease of use. Continual monitoring of the patient's physiological state with capabilities to provide drug intervention will greatly benefit the biomedical community. For example, Xiang and coworkers designed a flexible microfluidic drug patch for inflammation treatment [33]. The device comprises a micropump, microneedles, and microchannels preloaded with diclofenac. Even more recently, Lee et al.

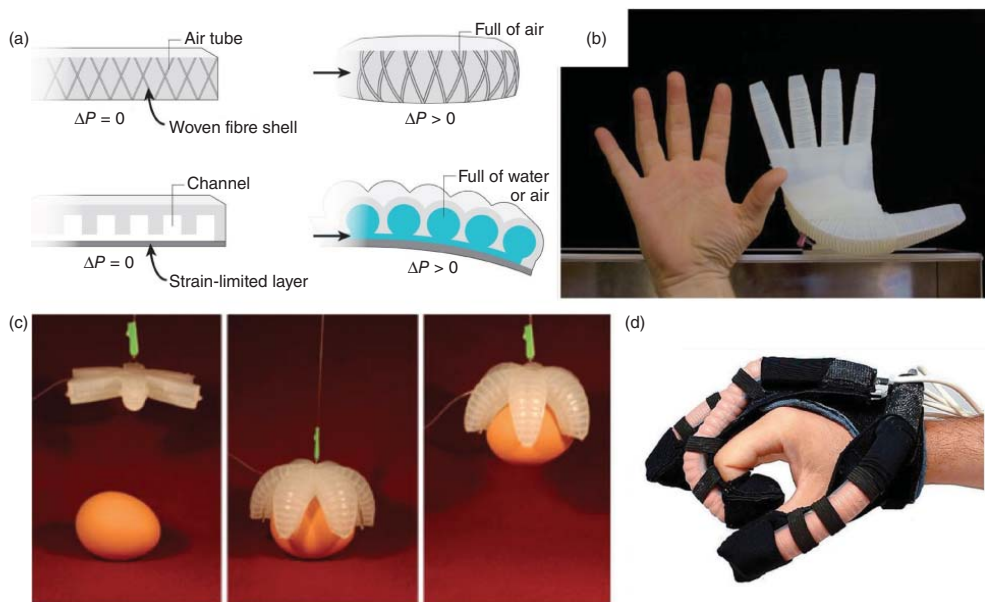


Figure 9.15 (a) Schematic illustration of the actuation mechanisms of microfluidics-based soft robotics [28]. (b) A compliant and underactuated robotic hand for dexterous grasping. (c) Simple gripper fabricated by soft lithography for handling fragile objects. (d) A soft robotic glove for combined assistance and at-home rehabilitation. (a–d) Rus and Tolley 2015 [28]. Copyright 2015, Reproduced with permission of Springer Nature.

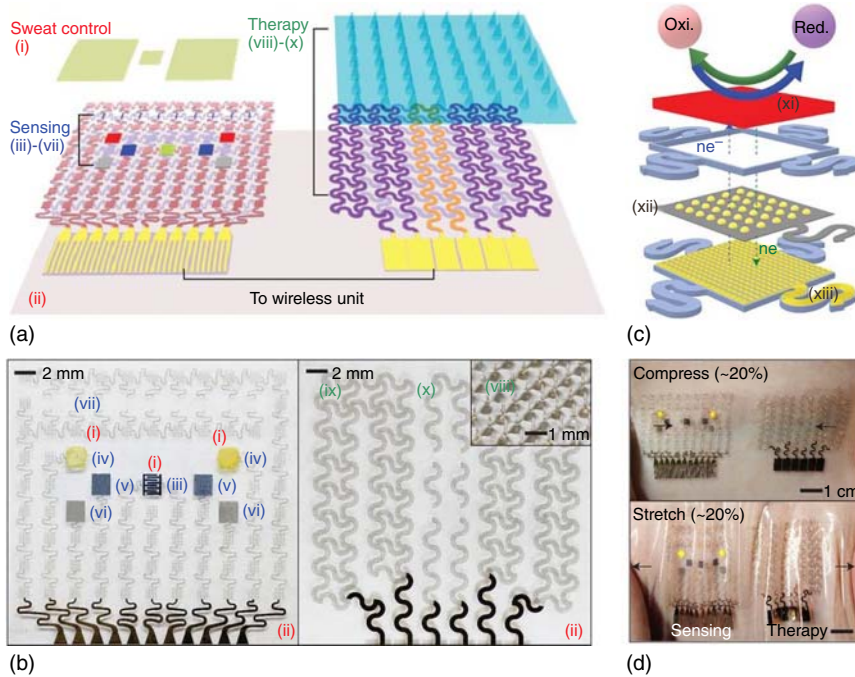


Figure 9.16 (a) Schematic drawings of the microfluidic drug patch. (b) Optical camera image of the electrochemical sensor array (left), therapeutic array (right), and magnified view of the drug-loaded microneedles (inset). (c) Schematic of the GP-hybrid electrochemical unit. (d) Optical camera images of the diabetes patch laminated on human skin under mechanical deformations. Source: (a–d) Lee et al. 2016 [34]. Copyright 2016, Reproduced with permission of Springer Nature.

developed a wearable patch that combines monitoring and intervention of diabetes through sweat analysis [34]. Figure 9.16a–c shows the schematic of the device layout. The patch comprises different functional elements, including temperature, humidity, glucose, and pH sensors, which allow complete glucose monitoring solutions. The device mounted on the skin could sustain conformability even under compression and tension (Figure 9.16d). Accordingly, glucose can be tracked continuously together with other variables and when abnormally high levels were detected, metformin may be administered to the skin through thermal activation via the microneedles on the sensor patch. Such proactive monitoring drug patches may potentially reduce catastrophic side effects and even save lives.

9.4.4.3 Implantable Devices

Flexible microfluidics is also suitable for implantable applications such as drug injection and status monitoring. Soft microfluidics could allow pharmacological infusions while minimizing tissue damage and inflammation, making long-term implantation possible. For instance, Jeong et al. developed a wireless optofluidic system that enabled programmable *in vivo* pharmacology and optogenetics, as shown in Figure 9.17 [35]. A neural probe composed of sufficiently thin and

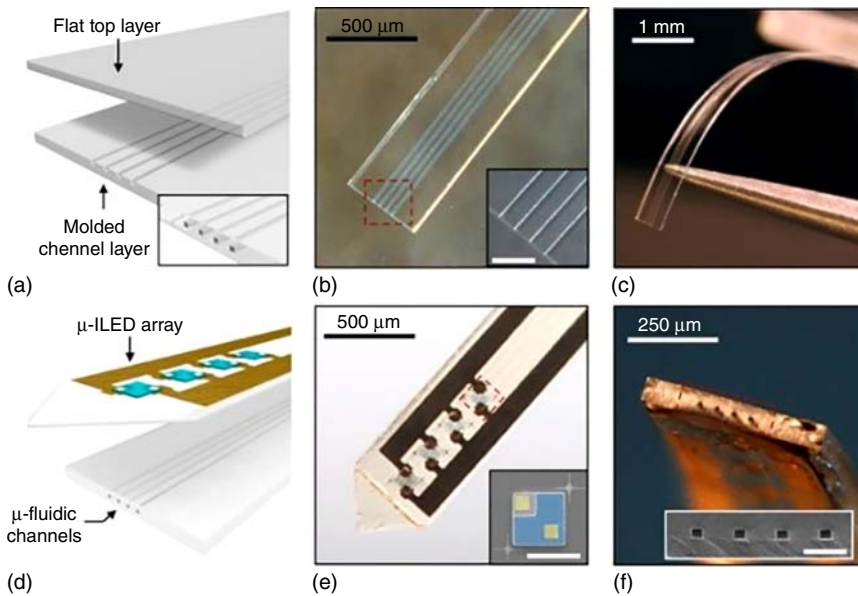


Figure 9.17 Schematic illustration and photographs of the optofluidic neuro probe. (a) Schematic diagram of the assembly of a soft microfluidic probe. (b) Optical micrograph of a microfluidic probe formed in this way. (Inset) Magnified view of the channels. Scale bar, 100 μm . (c) The picture that illustrates the soft, compliant mechanics of the device. (d) Schematic diagram of the integration of a soft microfluidic probe with a flexible array of μ -LEDs (light emitting diode) and metal interconnect traces on a film of PET. (e) Optical micrograph of an integrated probe, which was referred to as an optofluidic system. (Inset) Colorized SEM of a representative μ -ILED (inorganic light emitting diode). (f) Tilted view of an optofluidic probe that shows the tip end. (Inset) SEM of the outlets of the microfluidic channels. Source: (a–f) Jeong et al. 2015 [35]. Copyright 2015, Reproduced with permission of Elsevier.

flexible microfluidics could be implanted into the deep brain tissue region of rodents, which enabled wireless programmed spatiotemporal control of fluid delivery and photostimulation while having a size that is orders of magnitude smaller than conventional counterparts. The minimally invasive operation of these probes forecasts utility in other organ systems and species, with potential for broad application in biomedical science, engineering, and medicine.

9.4.4.4 Flexible Display

Flexible microfluidics has also been used for flexible display recently. Kobayashi and Onoe reported a multicolored flexible display based on sequentially introducing colored water droplets and air pockets into a microfluidic device fabricated with PDMS, as shown in Figure 9.18 [36]. The microfluidic device based on a flexible polymer enables a display with zero power consumption. Single water droplets define individual pixels, which are separated by air gaps; pumping water and air through the device in sequence allows colored patterns to be displayed, which can be controlled by varying the sequence of water and air, as well as water color. Additionally, retaining the pattern does not require the input of energy,

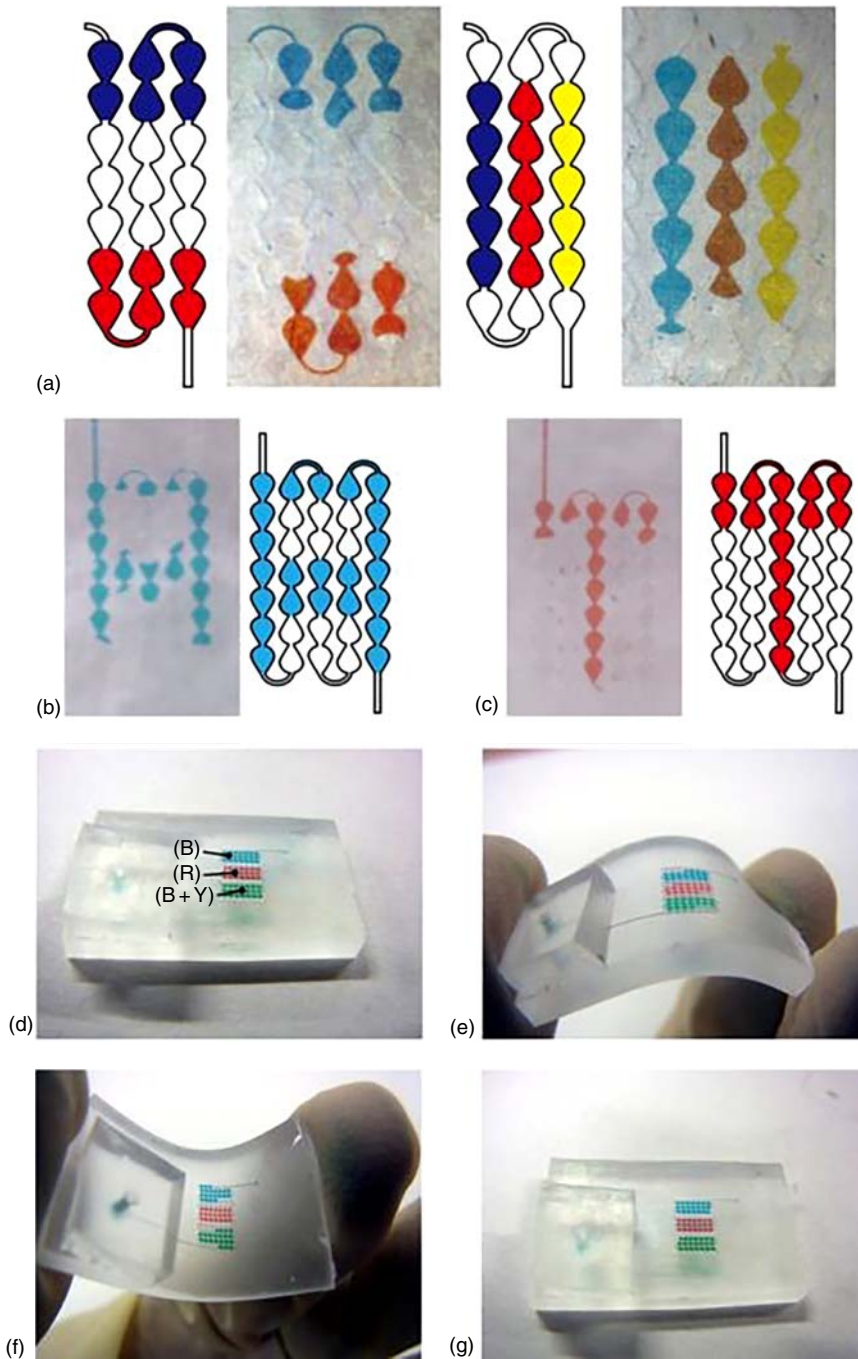


Figure 9.18 Demonstrations of the microfluidics-based flexible display. (a) Multicolored stripe patterns (vertical and horizontal) displayed on meandering microchannel. (b–c) Bitmap characters “A” and “T” on microfluidics-based reflective display. (d–g) Bending test of the display. The display image was maintained after the bending. Source: (a–g) Kobayashi and Onoe 2018 [36]. Copyright 2018, Reproduced with permission of Wiley-VCH Verlag GmbH & Co. KGaA. <https://www.nature.com/articles/s41378-018-0018-1#rightslink>. <http://creativecommons.org/licenses/by/4.0/>. Licensed under CC BY 4.0.

while PDMS makes the device flexible. Such a device could find application in displays on clothes and the skin of robots.

9.5 Challenges

In the future, more and more flexible materials with great physical properties, chemical stability, and biocompatibility will be developed. The emergence of novel materials and the development of fabrication technologies will promote the applications of flexible microfluidics in life science, health care, chemical analysis, and so on.

Further research and development are required to find better ways of packaging rigid, fragile sensors into the flexible microfluidic system. Flexible microfluidics can also benefit from the performance improvements of the sensors on flexible substrates. In addition, more robust and stable fluid manipulating and sensing components must be designed to enable long-term use.

References

- 1 Yeo, J.C., Kenry, K., and Lim, C.T. (2016). *Lab Chip* 16: 4082.
- 2 Metz, S., Holzer, R., and Renaud, P. (2001). *Lab Chip* 1: 29.
- 3 Liaw, D.-J., Wang, K.-L., Huang, Y.-C. et al. (2012). *Prog. Polym. Sci.* 37: 907.
- 4 Wang, S.Q., Chinnasamy, T., Lifson, M.A. et al. (2016). *Trends Biotechnol.* 34: 909.
- 5 Schubert-Ullrich, P., Rudolf, J., Ansari, P. et al. (2009). *Anal. Bioanal. Chem.* 395: 69.
- 6 Martinez, A.W., Phillips, S.T., Butte, M.J., and Whitesides, G.M. (2007). *Angew. Chem. Int. Ed.* 46: 1318.
- 7 Nguyen, N.T. (2008). *Micromixers*. Elsevier.
- 8 Kim, P., Kwon, K.W., Park, M.C. et al. (2008). *Biochip J.* 2: 1.
- 9 Guo, Y.Z., Li, L.H., Li, F.Y. et al. (2015). *Lab Chip* 15: 1759.
- 10 Saggiomo, V. and Velders, A.H. (2015). *Adv. Sci.*: 2.
- 11 Comina, G., Suska, A., and Filippini, D. (2014). *Lab Chip* 14: 424.
- 12 Martinez, A.W., Phillips, S.T., and Whitesides, G.M. (2008). *Proc. Natl. Acad. Sci. U.S.A.* 105: 19606.
- 13 Xing, S.Y., Jiang, J., and Pan, T.R. (2013). *Lab Chip* 13: 1937.
- 14 Heikenfeld, J. (2016). *Electroanalysis* 28: 1242.
- 15 Kim, S.B., Zhang, Y., Won, S.M. et al. (2018). *Small* 14: e1703334.
- 16 Koh, A., Kang, D., Xue, Y. et al. (2016). *Sci. Transl. Med.* 8: 366ra165.
- 17 Anastasova, S., Crewther, B., Bemnowicz, P. et al. (2017). *Biosens. Bioelectron.* 93: 139.
- 18 Benito-Lopez, F., Coyle, S., Byrne, R., and Diamond, D. (2001). Sensing sweat in real-time using wearable microfluidics. *Proceedings of the 7th International Workshop on Wearable and Implantable Body Sensor Networks*, Singapore (26–28 June 2010).
- 19 Yang, Y., Xing, S., Fang, Z. et al. (2017). *Lab Chip* 17: 926.

- 20 Yu, H., Li, D., Roberts, R.C. et al. (2012). *J. Microelectromech. Syst.* 21: 917.
- 21 Li, D., Lu, B., Zhu, R. et al. (2016). *Biomicrofluidics* 10: 011913.
- 22 Wu, J., Wang, R., Yu, H. et al. (2015). *Lab Chip* 15: 690.
- 23 Pu, Z., Wang, R., Wu, J. et al. (2016). *Sens. Actuators, B* 230: 801.
- 24 Pu, Z., Yu, H., Lai, X. et al. (2017). Flexible epidermal microfluidic system for continuous glucose monitoring. *The 21st International Conference on Miniaturized Systems for Chemistry and Life Sciences (MicroTAS 2017)*, Savannah, Georgia, USA (22–26 October 2017).
- 25 Yeo, J.C., Yu, J., Koh, Z.M. et al. (2016). *Lab Chip* 16: 3244.
- 26 Jiao, Y., Young, C.W., Yang, S. et al. (2016). *IEEE Sens. J.* 16: 7870.
- 27 Chossat, J., Yiwei, T., Duchaine, V., and Park, Y. (2015). Wearable soft artificial skin for hand motion detection with embedded microfluidic strain sensing. *2015 IEEE International Conference on Robotics and Automation (ICRA)*, Seattle, Washington, USA (26–30 May 2015).
- 28 Rus, D. and Tolley, M.T. (2015). *Nature* 521: 467.
- 29 Cianchetti, M., Laschi, C., Menciassi, A., and Dario, P. (2018). *Nat. Rev. Mater.* 3: 143.
- 30 Polygerinos, P., Wang, Z., Galloway, K.C. et al. (2015). *Rob. Autom. Syst.* 73: 135.
- 31 Deimel, R. and Brock, O. (2015). *Int. J. Rob. Res.* 35: 161.
- 32 Noh, Y., Sareh, S., Back, J. et al. (2014). *IEEE Int. Conf. Rob.:* 6388.
- 33 Wang, H., Xiang, Z., Giorgia, P. et al. (2016). *Nano Energy* 23: 80.
- 34 Lee, H., Choi, T.K., Lee, Y.B. et al. (2016). *Nat. Nanotechnol.* 11: 566.
- 35 Jeong, J.W., McCall, J.G., Shin, G. et al. (2015). *Cell* 162: 662.
- 36 Kobayashi, K. and Onoe, H. (2018). *Microsyst. Nanoeng.* 4: 1–11.